

# Direct Conversion of Fibroblasts into Stably Expandable Neural Stem Cells

Marc Thier,<sup>1,2,6</sup> Philipp Wörsdörfer,<sup>1,2,6</sup> Yenal B. Lakes,<sup>1,2,6</sup> Raphaela Gorris,<sup>2</sup> Stefan Herms,<sup>3</sup> Thoralf Opitz,<sup>4</sup> Dominic Seiferling,<sup>1,2</sup> Tamara Quandt,<sup>2</sup> Per Hoffmann,<sup>3</sup> Markus M. Nöthen,<sup>3,5</sup> Oliver Brüstle,<sup>2</sup> and Frank Edenhofer<sup>1,2,\*</sup>

<sup>1</sup>Stem Cell Engineering Group at the Institute of Reconstructive Neurobiology

<sup>2</sup>Institute of Reconstructive Neurobiology, Life & Brain Center, Hertie Foundation

<sup>3</sup>Institute of Human Genetics

<sup>4</sup>Department of Epileptology

University of Bonn, Sigmund-Freud Strasse 25, D-53105 Bonn, Germany

<sup>5</sup>German Center for Neurodegenerative Disorders (DZNE), Sigmund-Freud Strasse 25, D-53105 Bonn, Germany

<sup>6</sup>These authors contributed equally to this work

\*Correspondence: f.edenhofer@uni-bonn.de

DOI 10.1016/j.stem.2012.03.003

## SUMMARY

Recent advances have suggested that direct induction of neural stem cells (NSCs) could provide an alternative to derivation from somatic tissues or pluripotent cells. Here we show direct derivation of stably expandable NSCs from mouse fibroblasts through a curtailed version of reprogramming to pluripotency. By constitutively inducing Sox2, Klf4, and c-Myc while strictly limiting Oct4 activity to the initial phase of reprogramming, we generated neurosphere-like colonies that could be expanded for more than 50 passages and do not depend on sustained expression of the reprogramming factors. These induced neural stem cells (iNSCs) uniformly display morphological and molecular features of NSCs, such as the expression of Nestin, Pax6, and Olig2, and have a genome-wide transcriptional profile similar to that of brain-derived NSCs. Moreover, iNSCs can differentiate into neurons, astrocytes, and oligodendrocytes. Our results demonstrate that functional NSCs can be generated from somatic cells by factor-driven induction.

## INTRODUCTION

Forced expression of lineage-specific factors has been shown to reprogram the developmental plasticity of various somatic cell types (Graf and Enver, 2009; Yamanaka and Blau, 2010; Zhou and Melton, 2008). The seminal report describing induction of pluripotency in fibroblast cells represented a major breakthrough of cellular reprogramming (Takahashi and Yamanaka, 2006). Although substantial progress has been made in terms of improving the efficiency and robustness of reprogramming, the derivation of patient-specific iPSCs still is a lengthy and cumbersome procedure. Moreover, disease-related applications require subsequent redifferentiation into the desired cell type, and incomplete differentiation of iPSCs carries the risk of tumor induction by remaining undifferentiated iPSCs.

Recently, factor-driven reprogramming of fibroblasts has been reported to directly yield other somatic cell types such as neurons (Caiazzo et al., 2011; Pang et al., 2010; Pfisterer et al., 2011; Vierbuchen et al., 2010; Yoo et al., 2011), cardiomyocytes (Efe et al., 2011; Ieda et al., 2010), hepatocyte-like cells (Huang et al., 2011), blood (Szabo et al., 2010), and neural (Kim et al., 2011; Lujan et al., 2012) progenitors. These reports demonstrate that transdifferentiation from one differentiated cell type into another can be achieved through overexpression of transcription factors. However, transdifferentiation protocols published thus far result in somatic cell populations with little or no proliferation potential. Derivation of somatic stem cells would be highly desirable because such cells would be fully expandable and able to differentiate into multiple lineages in vitro and in vivo. Although neural stem cells (NSCs) can be derived from either somatic tissue or pluripotent sources (Conti et al., 2005; Tropepe et al., 2001; Uchida et al., 2000), the artificial induction of stably expandable NSCs has remained elusive. Here we show direct derivation of stably expandable NSCs from fibroblasts through a curtailed version of reprogramming toward pluripotency. Neurosphere-like colonies were isolated, and the resulting induced NSC (iNSC) lines maintained their tripotent developmental potential over prolonged expansion (>50 passages) and were not dependent on sustained expression of reprogramming factors.

## RESULTS

### Derivation of Neurosphere-like Clusters by Curtailed Reprogramming

Self-renewing NSCs can be derived from ESCs and fetal or adult forebrain (Uchida et al., 2000; Tropepe et al., 2001; Conti et al., 2005; Pollard et al., 2006). Such NSCs display many hallmarks of radial glia by morphology and molecular markers and are able to differentiate into neurons, astrocytes and oligodendrocytes. Because NSCs endogenously express a subset of iPSC reprogramming factors, namely Sox2, Klf4, and c-Myc, but not Oct4, we investigated whether curtailed reprogramming with restricted Oct4 activity could convert fibroblasts into NSCs. To test our hypothesis we infected mouse embryonic fibroblasts (MEFs) with retroviruses constitutively expressing

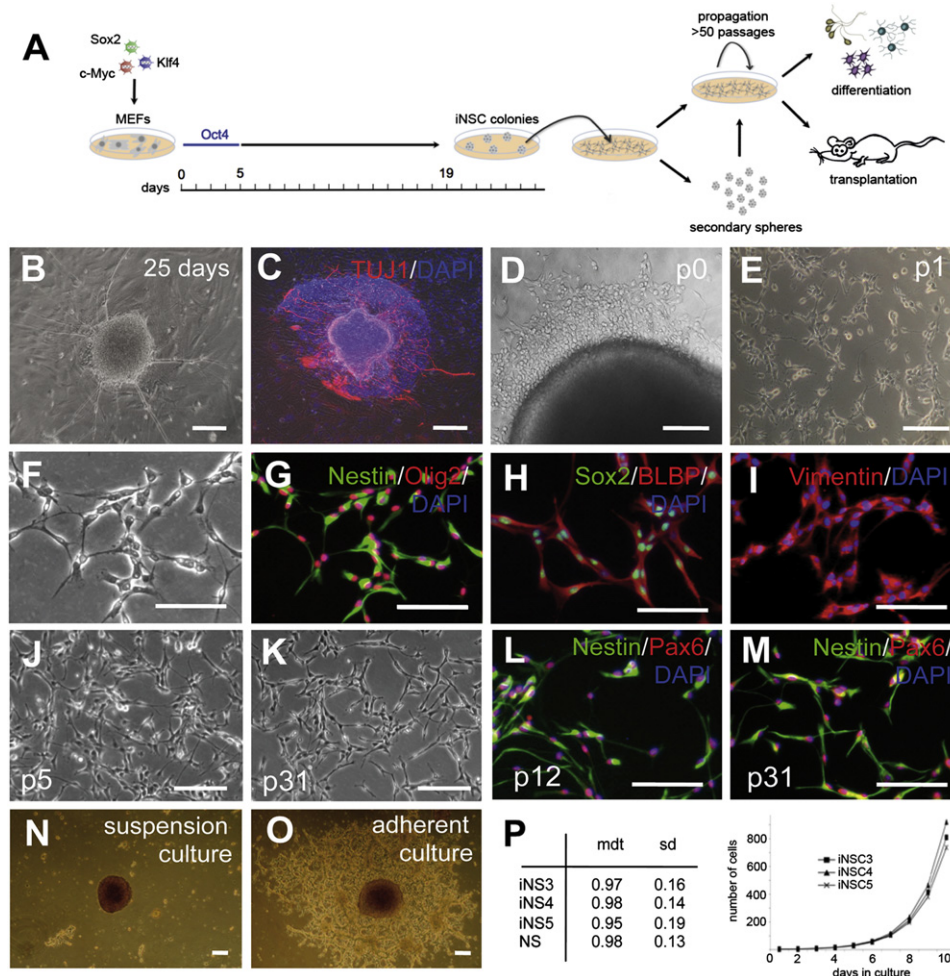


**Figure 1. Generation and Characterization of iNSCs from Mouse Embryonic Fibroblasts**

(A) Schematic drawing of the experimental setup and strategy to derive induced neural stem cells (iNSCs). (B) Neurosphere-like colony at day 25 with axonal structures processing out of the sphere. (C) Neurosphere-like colony at day 27 stained with a specific antibody directed against the neuronal marker  $\beta$ -III-tubulin. (D) Neurosphere-like colony isolated by manual picking, grown on a POL-coated culture dish. iNSCs are migrating out of the sphere (defined as passage 0). (E) iNSCs (passage 1) were dissociated to a single-cell suspension, seeded onto a POL-coated culture dish, and cultured for 2 days. (F–I) Immunofluorescence analysis of NSC marker proteins in iNSCs using specific antibodies directed to Nestin and Olig2 (G), Sox2 and BLBP (H), and mesenchymal marker Vimentin (I). A phase contrast micrograph is shown in (F). (J and K) Phase contrast pictures of iNSCs in NS propagation medium at passage 5 (J) and 31 (K). (L and M) iNSCs at passage 12 (L) and passage 31 (M) were stained for NSC markers Nestin and Pax6. (N and O) iNSCs form secondary neurospheres when kept in suspension culture (N). After plating on POL-coated culture dishes, spheres get adherent and iNSCs migrate out (O). (P) Mean doubling time (mdt) and growth curve of three iNSC lines (clone 3-5) in comparison to brain-derived NSCs (NS). sd, standard deviation.  $n = 6$ . Scale Bars: 50  $\mu$ m. See also Figure S1.

Sox2, Klf4, and c-Myc (SKC) (Figure 1A). To achieve control of Oct4 activity, we used a lentivirus enabling doxycycline (DOX)-controlled Oct4 activation (Soldner et al., 2009). We used media with reduced fetal calf serum (FCS, 2%) for transdifferentiation of fibroblast cells into NSCs because, although FCS is required for efficient propagation of fibroblasts, it induces unwanted terminal differentiation of NSCs. We compensated for the reduced serum content by applying serum replacement, which exhibits marginal effects only on NSC differentiation (data not shown). Approximately 130,000 Oct4-GiP (GFP-IRES-puro) reporter MEF cells

(Ying et al., 2002) were transduced and kept in the presence of DOX for up to 5 days to ensure expression of Oct4 temporarily and yet maintain the expression of the other three factors. Rare neurosphere-like colonies emerged that exhibited neither iPSC-like morphology nor GFP fluorescence by 11 days postinfection (p.i.). Cultures that had been treated with DOX for 5 days also yielded GFP-positive iPSC-like colonies. From this observation we concluded that a short and strictly regulated pulse of Oct4 expression is critical for NSC induction, but prolonged expression of Oct4 favors iPSC induction. Moreover, we

reasoned that the basal activity of the DOX system in the absence of the inducer does not allow a tightly regulated abrogation of Oct4 activation that is sufficient to impede terminal iPSC formation. Thus, we employed systems that enable more precise control over Oct4 activity and involve direct delivery of cell-permeant Oct4 protein (Bosnali and Edenhofer, 2008; Thier et al., 2010; Zhou et al., 2009) and mRNA (Warren et al., 2010), respectively. Five days of Oct4 protein transduction into 130,000 SKC-infected fibroblasts generated up to 11 GFP-negative neurosphere-like structures (Figure 1B). Staining of neurosphere-like colonies at the primary plate revealed  $\beta$ -III-tubulin-positive processes emanating from the colonies (Figure 1C). Similar structures were found in SKC-infected tail tip fibroblast cells transfected with Oct4-encoding mRNA (Figure S1 available online). The colonies were picked 18 days p.i. and plated in NS propagation medium. NSC-like cells grew out of the spheres (Figure 1D) and could be kept in adherent culture (Figure 1E).

### Artificially Induced iNSCs Are Similar to Brain-Derived NSCs

To investigate the identity of the induced NSCs (iNSCs), we performed comprehensive molecular characterization at the protein and mRNA level. Immunostaining revealed that the transdifferentiated cells consistently expressed numerous NSC markers including Nestin and Olig2 (Figures 1F and 1G), Sox2, and Blbp (Figure 1H). RT-PCR analyses of transdifferentiated cells confirmed transcription of *Pax6*, *Blbp*, and *Sox2* (Figure S1), all of which are characteristic markers of NSCs (Conti et al., 2005). Next we assessed the capability of iNSCs to self renew and grow clonally under proliferation conditions. We reproduced the derivation of iNSCs in three independent experiments, each employing 130,000 cells and yielding between 7 and 11 neurosphere-like structures. In total, we isolated five of these structures, and four of them could be stably expanded. All four iNS lines analyzed expressed NSC markers and were expandable for more than 50 passages without changes in their morphology and growth properties (Figures 1J–1O). The mean doubling times of iNSCs were found to be similar to that of brain-derived control NSCs (Figure 1P). The characteristic profile of NSC marker expression did not change after prolonged passaging as judged by staining for Pax6 and Nestin (Figures 1L and 1M). To assess the secondary neurosphere-forming potential of iNSCs, we generated single-cell suspensions that were cultured in uncoated flasks forming secondary neurospheres (Figure 1N) that were able to grow again in adherent culture (Figure 1O). Using this approach, more than 60% of the spheres could be expanded. In conclusion, fibroblast-derived transdifferentiated cells represent a homogenous proliferating cell population resembling a previously described radial glia NSC type (Conti et al., 2005).

### Genome-Wide Transcriptional Profiling of iNSCs and Transgene Silencing

To analyze the similarities between iNSCs and control NSCs, we generated comparative global gene expression data by microarray analysis. Scatter plots of the scores for MEFs and ESCs, respectively, versus iNSC-2 cells (Figures 2A and 2B) revealed a significant difference between iNSCs and their parental

MEFs and pluripotent cells. In contrast, iNSC-2 cells are very similar to the control NSC line (Figure 2C) and the sister clone iNSC-5 isolated from the same transdifferentiation experiment (Figure 2D). Hierarchical cluster analysis revealed a high degree of similarity between all NSC lines independent of their origin (Figure 2E). Although there are subtle differences in the global gene expression profiles of the three iNSC lines tested, all of them are clearly distinct from both MEFs and ESCs. One of the established iNSC lines (iNSC-2) is particularly similar to the NSC control line derived from fetal brain (Figures 2C, 2E, and 2F). Numerous genes known to be involved in NSC self-renewal or neural determination, such as *Foxg1*, *Nes*, *Bmi1*, and *Olig2*, are strongly upregulated in iNSCs and NSCs compared to MEF cells (Figure 2F). Transcription of several fibroblast-specific genes such as *Col1a1*, *Col3a1*, *Dkk3*, and *Thy1* is downregulated (Figure 2F), but there is also a subset of genes exhibiting similar expression in MEFs and iNSCs (Figure S2A), suggesting some residual fibroblast epigenetic memory. To examine whether iNSCs exhibit a regional identity, we selected region-specific transcription factors from the microarray data set and assessed them via RT-PCR analysis. Although both iNSC and NSC controls share high expression of some forebrain markers such as *Emx2*, *Foxg1*, and *Nr2e1*, they exhibit low expression of forebrain-specific *Emx1* (Figures S2B and S2C). Some mid/hindbrain-specific mRNAs including *Gbx2* and *Egr2* are highly abundant in contrast to Pax2, which exhibits low transcript levels. We found ventral markers *Olig2* and *Nkx2.2* highly expressed and low expression of dorsal markers *Pax3* and *Pax7*. In conclusion, like their counterparts derived from brain, iNSCs do not fully correlate with a specific regional identity but are mostly compatible with a ventral fore/mid/hind-brain fate.

Retroviral iPSC generation involves gradual silencing of reprogramming transgenes during the induction of pluripotency. In fact, transgene silencing is a prerequisite for normal differentiation of iPSCs (Brambrink et al., 2008). Recent publications suggest that the stability of transdifferentiated phenotypes, in contrast, appear to depend on the sustained overexpression of reprogramming transgenes (Ieda et al., 2010; Sheng et al., 2011). We thus asked whether the self-renewal capacity and cellular identity of iNSCs depends on sustained overexpression of the exogenous reprogramming transgenes. RT-PCR analyses revealed that none of the four iNSC lines analyzed expressed transgenic Sox2, Klf4, or c-Myc. However, all of the lines exhibited induction of endogenous Sox2 expression and no expression of endogenous Oct4 (Figure 2G). To verify the initial requirement for the transdifferentiation factors, we performed genomic PCR analyses and found that the four iNSC lines analyzed carry genomic integrations of all three reprogramming transgenes (Figure 2H).

### iNSCs Differentiate into Neurons, Astrocytes, and Oligodendrocytes

Next we set out to examine the developmental potential of iNSCs by assessing their capacity for differentiation into the three main neural lineages. Astrocytic differentiation of iNSCs was induced by exposure to FCS, yielding cells with astrocyte morphology that uniformly stain for glial fibrillary acidic protein (GFAP) (Figure 3A). To target differentiation of iNSCs toward

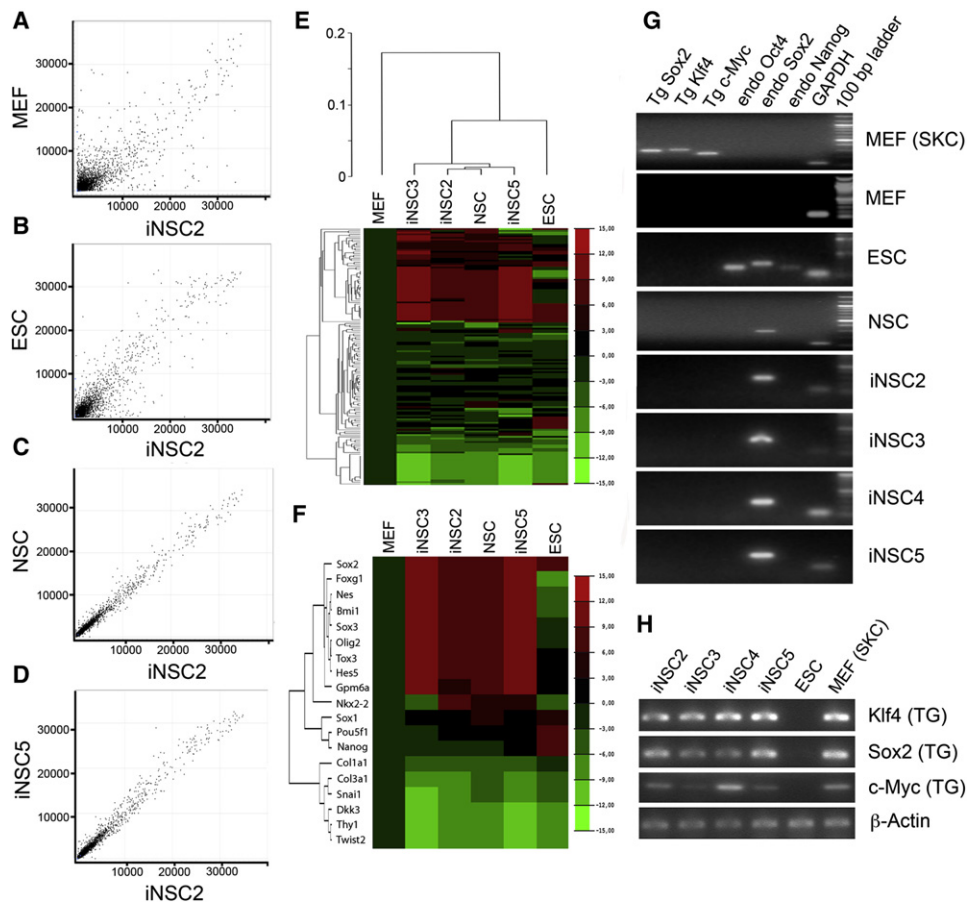


**Figure 2. Genome-Wide Transcriptional Profiling of iNSCs and Analysis of Transgene Silencing**

(A–D) Homogeneity of gene expression visualized by scatter plot presentation. Shown are plots of the averaged intensities of each group against the induced NSC clone 2 (iNSC2). Detection p values are  $\leq 0.01$ .

(E and F) Hierarchical cluster analysis and heatmap presentation of microarray expression analysis of MEF cells, three iNSC lines (iNSC2, 3, 5), NS control cells (NSC), and ESCs (ESC). All samples had been processed in at least triplicate to reduce signals arising from processing artifacts. Plotted are the differential score values of 147 genes selected by text-mining for the term “neuro” in the gene definition data provided by GenomeStudio (E) and a subset of selected neural, pluripotency, and fibroblast-specific genes (F) as computed by GenomeStudio’s differential gene analysis algorithm.

(G) RT-PCR analyses of four iNSC lines (clone 2–5) for sustained expression of the retroviral transgenes as well as endogenous expression of Oct4, Sox2, and Nanog. RNA preparations of uninfected MEFs, SKC-infected MEFs (SKC), and ESCs as well as a brain-derived NSC line serve as controls. All four iNSC lines analyzed exhibit expression of endogenous Sox2 like the NSC sample. Transcription of transgenic factors was not observed. Primer pair detecting the glyceraldehyde 3-phosphate dehydrogenase (GAPDH) is used as loading control.

(H) Genomic PCR to verify integration of retroviral constructs used for partial reprogramming. Primer pair detecting endogenous  $\beta$ -actin serve as loading control. See also Figure S2.

the oligodendroglial fate, we used a protocol employing media containing forskolin, triiodothyronine, and ascorbic acid. Staining revealed oligodendrocyte marker O4-positive cells with characteristic morphology (Figure 3B). For neuronal differentiation iNSCs were cultivated in the absence of EGF/FGF but in the presence of BDNF. Differentiated cells showed neuronal morphology and expression of the neuronal markers  $\beta$ -III-tubulin (Figure 3C) and NeuN (Figures 3D and 3E) as well as microtubule-associated protein (MAP2) (Figures 3C and 3F). Quantification of the differentiated cells demonstrated that the differentiation potential of iNSCs is high for astrocytes and neurons whereas oligodendroglial differentiation is relatively rare (Figure 3G). Thus, iNSCs are very similar to their counterparts derived from brain tissue for which oligodendrocyte differentiation is challenging (Figure S3A) (Conti et al., 2005; Glaser et al., 2007).

Nevertheless, the differentiation spectrum of iNSCs is not restricted to neurons and astrocytes but extends also to oligodendrocytes. All four iNSC lines analyzed exhibit a similar potential to differentiate into neurons (Figure S3B). Further cellular characterization of iNSC-derived neurons revealed that the majority developed a GABAergic phenotype (Figure 3H) and some are able to express synaptic proteins (Figure 3I). To analyze whether the resulting neurons exhibit functional membrane properties, we performed whole-cell patch-clamp recordings after 3 weeks of differentiation. This analysis revealed the expression of a complex outward current pattern including inactivating and sustained components (Figure 3J). This pattern is reminiscent of neurons expressing both A-type and delayed rectifier potassium channels. In contrast to these high-amplitude outward currents, transient inward currents were only of small



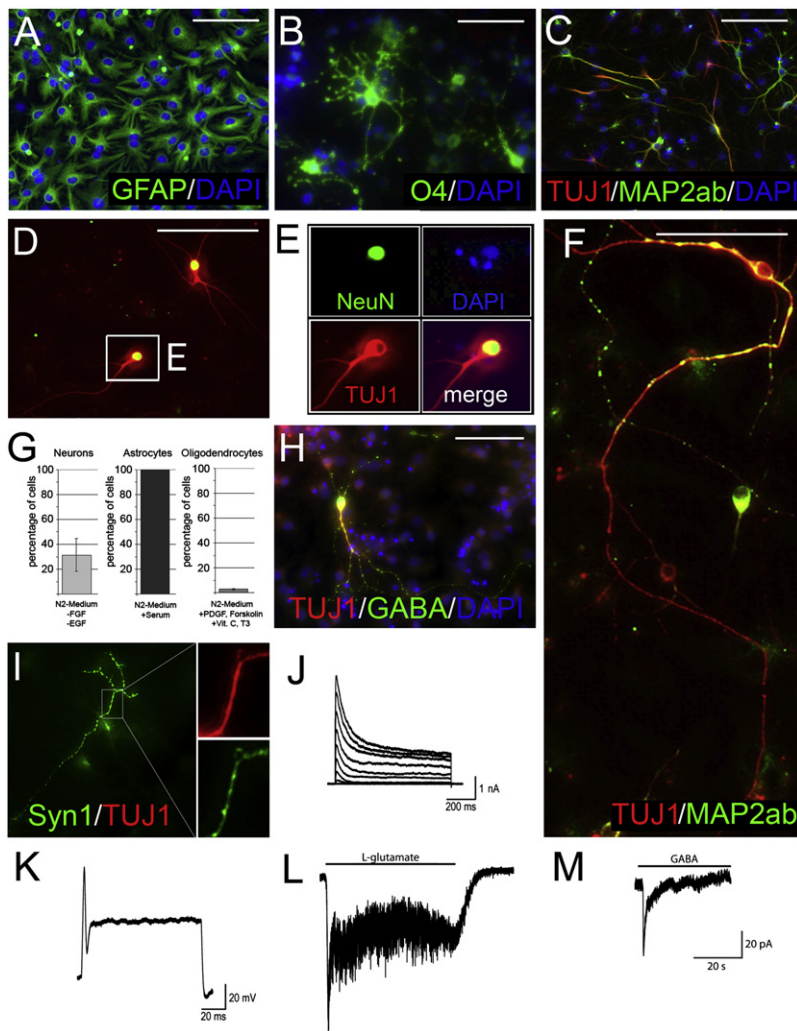


**Figure 3. In Vitro Differentiation Potential of iNSCs**

(A–C) iNSCs differentiate into astrocytes, oligodendrocytes, and neurons in vitro as judged by immunofluorescence analyses using specific antibodies directed against GFAP, O4,  $\beta$ -III-tubulin, and MAP2ab.

(D and E) iNSC-derived neurons stain positive for the neuron-specific marker NeuN. (E) shows a magnification of (D).

(F and H) iNSC-derived neurons expressing the mature neuronal marker MAP2ab and GABA, respectively.

(G) Quantification of the differentiation potential of iNSCs into neurons, astrocytes, and oligodendrocytes. About 30% of the iNSC-derived progeny stain TUJ1-positive when cultured in N2 medium without EGF and bFGF. In serum-containing medium, almost 100% of the cells differentiate into astrocytes. About 3% oligodendrocytes are found after culture in N2 medium with PDGF, Forskolin, and T3 followed by N2 medium with ascorbic acid. (I) Staining of iNSC-derived neurons for Synapsin and  $\beta$ -III-tubulin after three weeks of differentiation.

(J–M) Physiological properties of iNSC-derived neurons assessed by whole-cell patch-clamp recordings. (J) Complex outward current pattern including inactivating and sustained components reminiscent of neurons expressing both A-type and delayed rectifier potassium channels. (K) Current-clamp experiment of an iNSC-derived neuron able to fire an action potential, thus demonstrating membrane excitability. (L and M) Local application of either 15 mM L-glutamate (L) or 15 mM GABA (M) elicited a clear current response, indicating the expression of functional neurotransmitter receptors ( $n = 5$  and  $3$ , respectively). Stainings were performed after 2 weeks of differentiation if not otherwise stated. Recordings were done after 3 weeks.

Scale bars: 50  $\mu$ m. See also Figure S3.

amplitude. However, in current-clamp experiments some cells (five of seven) were able to fire an action potential, demonstrating membrane excitability (Figure 3K). Furthermore, the neurons displayed surface expression of glutamate and GABA<sub>A</sub> receptors ( $n = 5$  and  $n = 3$ , respectively, Figures 3L and 3M), which is a prerequisite for the formation of glutamatergic and GABAergic synapses.

Finally, we conducted first studies to assess the in vivo developmental potential of iNSCs. Specifically, we wanted to explore whether iNSCs might be suitable for glial cell replacement. To address this question, we transplanted them into the brain of neonatal myelin-deficient (md) rats. Cells were transplanted into the left and right hemispheres and 2 weeks later detected by staining against the murine neural marker M2 and oligodendroglial proteolipid protein (PLP), which is deficient in the md rat brain. These in vivo studies revealed iNSC-derived M2-positive cells with astrocyte morphology in a variety of host brain regions including cortex and striatum (Figure 4). Many of the M2-positive profiles could be double-labeled with an antibody to GFAP (Figures 4B and 4C). In addition, PLP-positive profiles were detected in white matter structures such as the corpus callosum (Figure 4D). While these

data need to be complemented by other glial markers and an assessment of in vivo neuronal differentiation, they clearly demonstrate that grafted iNSCs survive and give rise to differentiated neural cells in vivo.

## DISCUSSION

Our data demonstrate the induction of stably expandable iNSCs from fibroblasts using a curtailed version of reprogramming toward pluripotency. iNSCs uniformly exhibit morphological and molecular features of NSCs such as the expression of Nestin, Olig2, Sox2, Blbp, and Pax6. Genome-wide transcriptional profiling confirms a high degree of similarity between artificially induced NSCs and their counterparts derived from mouse brain. Moreover, we demonstrate tripotential differentiation capacity of iNSCs into the three main neural lineages. Notably, iNSCs are able to generate primary and secondary neurospheres and maintain their marker expression profile and differentiation capacity over prolonged expansion (>50 passages). The uniformity and stability of growth characteristics and marker expression together with long-term maintenance of tripotential neural differentiation capability suggest that iNSCs represent a stably proliferating somatic stem cell type. Thus, in conclusion, iNSCs show

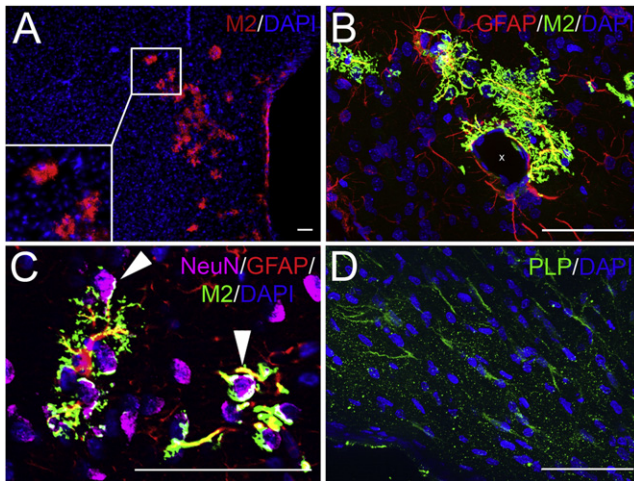


**Figure 4. Transplantation of iNSCs into the Brains of Neonatal Rats**  
iNSCs were transplanted into the left and right hemispheres of postnatal myelin-deficient rats. Two weeks after transplantation rats were sacrificed and brain slices were analyzed.

(A) M2 antibody marks murine iNSC-derived mouse cells integrated into the rat brain.

(B–D) Immunofluorescence analyses using specific antibodies targeted against astrocyte-specific GFAP (B and C), neuron-specific NeuN (C), and oligodendrocyte-specific PLP (D). M2/GFAP double-positive mouse astrocytes are found in close contact with a blood vessel. The white x in (B) indicates the lumen of the vessel. Arrowheads in (C) point to iNSC-derived M2/GFAP double-positive astrocyte processes that surround host neurons.

Scale bars: 50  $\mu$ m.

the cardinal features of NSCs: self-renewal and neural multipotentiality.

Recent studies have shown that direct conversion of fibroblasts into other somatic cell types including neurons (Caiazzo et al., 2011; Pang et al., 2010; Pfisterer et al., 2011; Vierbuchen et al., 2010; Yoo et al., 2011) and neural progenitors (Kim et al., 2011; Lujan et al., 2012) is feasible. Kim et al. recently reported the direct reprogramming of fibroblasts to neural progenitor cells (NPCs) by employing DOX-controlled overexpression of Oct4, Sox2, Klf4, and c-Myc. The authors demonstrate that differentiation of such transdifferentiated NPCs yields neurons and astrocytes. The oligodendrocyte differentiation capability remained unclear, however. Moreover, the NPCs were reported to lose their ability to form colonies within three to five passages (Kim et al., 2011). Our data demonstrate that iNSCs, by contrast, are stably expandable (thus far for more than 50 passages) and exhibit tripotential neural differentiation. We deliberately used a regulated system for Oct4 while constitutively inducing activity of the other three factors (Sox2, Klf4, and c-Myc) that are expressed endogenously in NSCs. We reasoned that this approach could combine strong neuroinductive capacity from high levels of Sox2, Klf4, and c-Myc, but reduced induction of pluripotency through limiting the expression of Oct4. In this regard, Oct4 protein transduction or mRNA transfection may be preferable to transcriptional control due to the leakage of basal Oct4 expression in the absence of inducer. Temporary use of cell-permeant Oct4 protein allows precise and unambiguous cessation of Oct4 reprogramming activity.

The transcriptional activity of viral transgenes in reprogrammed cells represents a critical issue. While conventional iPSC generation requires transgene silencing, recently published transdifferentiation studies report incomplete silencing of reprogramming genes, indicating that sustained expression of exogenous genes is necessary for the maintenance of the reprogrammed phenotype (leda et al., 2010; Sheng et al., 2011). Employing the transdifferentiation paradigm described in this study, we demonstrate that the three transgenes needed (Klf4, c-Myc, Sox2) are silenced in all derived iNSC lines analyzed. Concomitantly, we show that endogenous Sox2 is upregulated in iNSCs. In conclusion, we show that self-renewal of iNSCs does not depend on sustained transgene expression, but seems to be triggered by activation of the intrinsic NSC transcriptional program as indicated by the switch from exogenous overexpression of Sox2 to efficient expression of endogenous Sox2. Additionally, this finding suggests that it may be possible to use entirely transgene-free approaches to derive iNSCs by delivering Klf4, c-Myc, and Sox2 using mRNA or proteins. Future studies remain to be done to adapt this iNSC protocol to human cells and to eventually substitute viral Sox2, Klf4, and c-Myc with nonintegrating delivery modes or small molecules. We anticipate that iNSCs could provide a safe and robust cellular platform for the generation of patient-specific neural cells for biomedical applications.

## EXPERIMENTAL PROCEDURES

### Cell Culture and Infection

Oct4-GiP MEFs (Ying et al., 2002) were infected with retroviruses encoding for Sox2, Klf4, and c-Myc. For tet-controlled experiments, MEFs were infected with lentiviruses FUW-Oct4 and M2rtTA (Soldner et al., 2009), which was followed by a second infection with retroviruses encoding for Sox2, Klf4, and c-Myc (Takahashi and Yamanaka, 2006). Oct4-TAT protein (Bosnali and Edenhofer, 2008) and 2  $\mu$ g/ml DOX (Sigma, Saint Louis, MO) were applied after the virus-containing supernatant had been removed. Experiments were carried out in iNSC induction medium (DMEM/F12, 2% FCS, 8% Serum Replacement, 1x N2, 2 mM L-glutamine, 100  $\mu$ M  $\beta$ -mercaptoethanol, 1x NEAA and 1000 U/ml ESGRO; all media and cell culture supplements were purchased from Life technologies, Carlsbad, CA, if not otherwise stated). After 18–22 days neurosphere-like colonies were picked, transferred to Polyornithine/Laminin (POL)-coated culture dishes, and kept in NS propagation medium (EuroMed-N, EuroClone, Sizzano, Italy), 1x N2, 10 ng/ml bFGF, and 10 ng/ml EGF (R&D Systems, Minneapolis, MN). iNSCs were characterized by RT-PCR analyses, immunofluorescence staining, and microarray analyses as given in the Supplemental Information.

### iNSC Differentiation

For the generation of astrocytes, iNSCs were kept in 10% FCS-containing medium supplemented with 1x NEAA and 2 mM L-glutamine. For neuronal differentiation iNSCs were plated onto POL-coated dishes and kept in a 1:1 mix of Neurobasal Medium and DMEM/F12 supplemented with N2, B27, and 10 ng/ml BDNF, as well as 200  $\mu$ M ascorbic acid (Sigma, Saint Louis, MO). Half of the medium was replaced every other day. After 2 weeks of culture, the ratio was changed to 3:1 and N2 supplement was reduced to 0.5%, while BDNF was increased to 20 ng/ml. To derive oligodendrocytes, iNSCs were cultivated in DMEM/F12 with 1x N2, 10 ng/ml PDGF (R&D Systems, Minneapolis, MN), and 10  $\mu$ M forskolin (Sigma, Saint Louis, MO) for 4 days. Afterwards, PDGF and forskolin were replaced by 30 ng/ml 3,3',5'-triiodothyronine (T3) hormone and 200  $\mu$ M ascorbic acid (all from Sigma, Saint Louis, MO) for another 7 days.

### Analysis of Transplanted iNSCs

Cells were transplanted into postnatal md rats (kind gift of Ian Duncan) as described previously (Glaser et al., 2007). Brain slices were incubated with

primary antibodies targeted against PLP (rb; 1:100, Abcam, Cambridge, UK), M2 (rat; 1:250, Developmental Studies Hybridoma Bank, Iowa City, IO), NeuN (ms; 1:50, Millipore, Billerica, MA), and GFAP (rb; 1:1,000; DAKO, Hamburg, Germany) overnight at room temperature. Alexa 488-, Cy3-, and Cy5-conjugated secondary antibodies were used (4 hr at room temperature) for visualization. Pictures were taken using a Zeiss Apotome microscope and an AxioVision camera (Carl Zeiss, Jena, Germany).

#### ACCESSION NUMBERS

The accession number for the microarray data reported here is GSE36484.

#### SUPPLEMENTAL INFORMATION

Supplemental Information for this article includes three figures, one table and Supplemental Experimental Procedures and can be found with this article online at doi:10.1016/j.stem.2012.03.003.

#### ACKNOWLEDGMENTS

We thank Austin Smith (Cambridge University, UK) for providing us with the Oct4-GiP reporter and NS5 cell line and Rudolf Jaenisch (Whitehead Institute, USA) for the kind gift of FUW-vectors. We are indebted to Ian Duncan (University of Wisconsin, USA) for providing us with md rats, Didier Trono (EPFL Lausanne, Switzerland) for providing the helper plasmids psPAX2 and pMD2.G, and Shinya Yamanaka for providing the plasmids pMXs-Sox2, pMXs-Klf4, and pMXs-c-myc. We thank Sandra Meyer and Rajkumar Thummer for critical reading of the manuscript; and Benedikt Berninger (Ludwig-Maximilians University Munich, Germany), Magdalena Götz (Institute for Stem Cell Research Munich, Germany), Veit Hornung (University of Bonn, Germany), and all members of the Stem Cell Engineering Group for helpful discussions. We thank Nicole Russ, Kathrin Vogt, Stephanie Mielke, and Anke Leinhaas for excellent technical support. This work was supported by grants from the Deutsche Forschungsgemeinschaft DFG (ED79/1-2), the German Ministry of Education and Research, BMBF (NewNeurons; 01GN1009B), the European Commission, and Merck KGaA, Darmstadt, Germany.

Received: July 18, 2011

Revised: January 25, 2012

Accepted: March 11, 2012

Published online: March 22, 2012

#### REFERENCES

- Bosnali, M., and Edenhofer, F. (2008). Generation of transducible versions of transcription factors Oct4 and Sox2. *Biol. Chem.* 389, 851–861.
- Brambrink, T., Foreman, R., Welstead, G.G., Lengner, C.J., Wernig, M., Suh, H., and Jaenisch, R. (2008). Sequential expression of pluripotency markers during direct reprogramming of mouse somatic cells. *Cell Stem Cell* 2, 151–159.
- Caiazzo, M., Dell'Anno, M.T., Dvoretzskova, E., Lazarevic, D., Taverna, S., Leo, D., Sotnikova, T.D., Menegon, A., Roncaglia, P., Colciago, G., et al. (2011). Direct generation of functional dopaminergic neurons from mouse and human fibroblasts. *Nature* 476, 224–227.
- Conti, L., Pollard, S.M., Gorba, T., Reitano, E., Toselli, M., Biella, G., Sun, Y., Sanzone, S., Ying, Q.L., Cattaneo, E., and Smith, A. (2005). Niche-independent symmetrical self-renewal of a mammalian tissue stem cell. *PLoS Biol.* 3, e283.
- Efe, J.A., Hilcove, S., Kim, J., Zhou, H., Ouyang, K., Wang, G., Chen, J., and Ding, S. (2011). Conversion of mouse fibroblasts into cardiomyocytes using a direct reprogramming strategy. *Nat. Cell Biol.* 13, 215–222.
- Glaser, T., Pollard, S.M., Smith, A., and Brüstle, O. (2007). Tripotential differentiation of adherently expandable neural stem (NS) cells. *PLoS ONE* 2, e298.
- Graf, T., and Enver, T. (2009). Forcing cells to change lineages. *Nature* 462, 587–594.
- Huang, P., He, Z., Ji, S., Sun, H., Xiang, D., Liu, C., Hu, Y., Wang, X., and Hui, L. (2011). Induction of functional hepatocyte-like cells from mouse fibroblasts by defined factors. *Nature* 475, 386–389.
- leda, M., Fu, J.D., Delgado-Olguin, P., Vedantham, V., Hayashi, Y., Bruneau, B.G., and Srivastava, D. (2010). Direct reprogramming of fibroblasts into functional cardiomyocytes by defined factors. *Cell* 142, 375–386.
- Kim, J., Efe, J.A., Zhu, S., Talantova, M., Yuan, X., Wang, S., Lipton, S.A., Zhang, K., and Ding, S. (2011). Direct reprogramming of mouse fibroblasts to neural progenitors. *Proc. Natl. Acad. Sci. USA* 108, 7838–7843.
- Lujan, E., Chanda, S., Ahlenius, H., Südhof, T.C., and Wernig, M. (2012). Direct conversion of mouse fibroblasts to self-renewing, tripotent neural precursor cells. *Proc. Natl. Acad. Sci. USA* 109, 2527–2532.
- Pang, Z.P., Yang, N., Vierbuchen, T., Ostermeier, A., Fuentes, D.R., Yang, T.Q., Citri, A., Sebastiano, V., Marro, S., Südhof, T.C., et al. (2010). Induction of human neuronal cells by defined transcription factors. *Nature* 476, 220–223.
- Pfisterer, U., Kirkeby, A., Torper, O., Wood, J., Nelander, J., Dufour, A., Björklund, A., Lindvall, O., Jakobsson, J., and Parmar, M. (2011). Direct conversion of human fibroblasts to dopaminergic neurons. *Proc. Natl. Acad. Sci. USA* 108, 10343–10348.
- Pollard, S.M., Conti, L., Sun, Y., Goffredo, D., and Smith, A. (2006). Adherent neural stem (NS) cells from fetal and adult forebrain. *Cereb. Cortex* 16 (Suppl 1), i112–i120.
- Sheng, C., Zheng, Q., Wu, J., Xu, Z., Wang, L., Li, W., Zhang, H., Zhao, X.Y., Liu, L., Wang, Z., et al. (2011). Direct reprogramming of Sertoli cells into multipotent neural stem cells by defined factors. *Cell Res.* 22, 208–218.
- Soldner, F., Hockemeyer, D., Beard, C., Gao, Q., Bell, G.W., Cook, E.G., Hargus, G., Blak, A., Cooper, O., Mitalipova, M., et al. (2009). Parkinson's disease patient-derived induced pluripotent stem cells free of viral reprogramming factors. *Cell* 136, 964–977.
- Szabo, E., Rampalli, S., Risueño, R.M., Schnerch, A., Mitchell, R., Fiebig-Comyn, A., Leivadoux-Martin, M., and Bhatia, M. (2010). Direct conversion of human fibroblasts to multilineage blood progenitors. *Nature* 468, 521–526.
- Takahashi, K., and Yamanaka, S. (2006). Induction of pluripotent stem cells from mouse embryonic and adult fibroblast cultures by defined factors. *Cell* 126, 663–676.
- Thier, M., Münst, B., and Edenhofer, F. (2010). Exploring refined conditions for reprogramming cells by recombinant Oct4 protein. *Int. J. Dev. Biol.* 54, 1713–1721.
- Tropepe, V., Hitoshi, S., Sirard, C., Mak, T.W., Rossant, J., and van der Kooy, D. (2001). Direct neural fate specification from embryonic stem cells: a primitive mammalian neural stem cell stage acquired through a default mechanism. *Neuron* 30, 65–78.
- Uchida, N., Buck, D.W., He, D., Reitsma, M.J., Masek, M., Phan, T.V., Tsukamoto, A.S., Gage, F.H., and Weissman, I.L. (2000). Direct isolation of human central nervous system stem cells. *Proc. Natl. Acad. Sci. USA* 97, 14720–14725.
- Vierbuchen, T., Ostermeier, A., Pang, Z.P., Kokubu, Y., Südhof, T.C., and Wernig, M. (2010). Direct conversion of fibroblasts to functional neurons by defined factors. *Nature* 463, 1035–1041.
- Warren, L., Manos, P.D., Ahfeldt, T., Loh, Y.H., Li, H., Lau, F., Ebina, W., Mandal, P.K., Smith, Z.D., Meissner, A., et al. (2010). Highly efficient reprogramming to pluripotency and directed differentiation of human cells with synthetic modified mRNA. *Cell Stem Cell* 7, 618–630.
- Yamanaka, S., and Blau, H.M. (2010). Nuclear reprogramming to a pluripotent state by three approaches. *Nature* 465, 704–712.
- Ying, Q.L., Nichols, J., Evans, E.P., and Smith, A.G. (2002). Changing potency by spontaneous fusion. *Nature* 416, 545–548.
- Yoo, A.S., Sun, A.X., Li, L., Shcheglovitov, A., Portmann, T., Li, Y., Lee-Messer, C., Dolmetsch, R.E., Tsien, R.W., and Crabtree, G.R. (2011). MicroRNA-mediated conversion of human fibroblasts to neurons. *Nature* 476, 228–231.
- Zhou, Q., and Melton, D.A. (2008). Extreme makeover: converting one cell into another. *Cell Stem Cell* 3, 382–388.
- Zhou, H., Wu, S., Joo, J.Y., Zhu, S., Han, D.W., Lin, T., Trauger, S., Bien, G., Yao, S., Zhu, Y., et al. (2009). Generation of induced pluripotent stem cells using recombinant proteins. *Cell Stem Cell* 4, 381–384.